International Journal of Mass Spectrometry 279 (2009) 119–125

Contents lists available at ScienceDirect

International Journal of Mass Spectrometry

journal homepage: www.elsevier.com/locate/ijms

Temperature effects in differential mobility spectrometry

Evgeny V. Krylov*, Stephen L. Coy, Erkinjon G. Nazarov

Sionex Corporation 8-A Preston Court, Bedford, MA 01730, USA

ARTICLE INFO

Article history:
Received 5 February 2008
Accepted 27 October 2008
Available online 12 November 2008

Keywords:
DMS
FAIMS
Effective temperature
Ion mobility

ABSTRACT

Drift gas temperature and pressure influence differential mobility spectrometer (DMS) performance, changing DMS peak positions, heights and widths. This study characterizes the effect of temperature on DMS peak positions. Positive ions of methyl salicylate, DMMP, and toluene, and negative ions of methyl salicylate and the reactant ion peaks were observed in purified nitrogen in the Sionex microDMx planar DMS. Measurements were made at ambient pressure (1 atm) at temperatures from 25 °C to 150 °C in a planar sensor with height 0.5 mm. Peak value of the separation voltage asymmetric waveform was scanned from 500 V to 1500 V. Compensation voltage (DMS peak position) showed a strong variation with temperature for all investigated ions. By generalizing the concept of effective ion temperature to include the effects of inelastic ion–molecular collisions, we have been able to condense peak position dependence on separation field and temperature to dependence on a redefined effective temperature including a smoothly varying inelasticity correction. It allows prediction and correction of the gas temperature effect on DMS peak positions.

Differential mobility spectrometry (DMS) [1–3] is recognized as a powerful tool for separation and characterization of gas-phase ions. In DMS, ions are distinguished by the difference between mobilities at high and low electric fields, exploiting the fact that ion mobility values depend on the applied field strength. Developed and refined over the past decade, DMS is also known as field-asymmetric waveform ion mobility spectrometry (FAIMS) [4] (FAIMS is often used to refer to a coaxial configuration). Several configurations of DMS analyzers have shown response to trace amounts of chemical species including explosives [5,6], chemical warfare agents and simulants [7], volatile organic compounds [8], and a variety of other organic and inorganic substances [9]. Hybrid DMS techniques such as GC–DMS [10], DMS–IMS [11], DMS–MS [12] and ESI–DMS–MS [13,14] can provide detection and identification traces of chemicals for many applications, including biomarkers and biological materials [15].

Stability and repeatability of DMS spectra are important issues in the use of DMS in analytical applications. Drift gas pressure and temperature are known to influence the field dependence of ion mobility, changing peak positions in DMS spectra. This study characterizes the effects of temperature on differential ion mobility and differential mobility spectrum peak position for several typical ion species. The findings provide deeper understanding of the role of the drift gas temperature in interactions between molecular ions and neutrals and the temperature effect on DMS separation. These results allow the development of algorithms to account for the influence of the drift gas conditions that will improve DMS performance under varying environmental conditions.

Pressure and temperature effects on DMS parameters are especially relevant to applications such at the use of planar DMS as an ion prefilter for mass spectrometric analysis. Including a compact planar DMS ion filter in the interface area of the API-MS instrument reduces spectral complexity and suppresses chemical noise, resulting in lower detection levels and better quantitation accuracy [16].

We previously found [17] that pressure variation of DMS peak positions may be eliminated by a rescaling of the coordinates, expressing both compensation and separation fields in Townsend units (electric field divided by density). At fixed temperature, Townsend-rescaled DMS spectra are independent of the drift gas pressure (see Fig. 1a). In contrast, DMS spectra recorded at fixed pressure but varying temperature do not simplify in a similar way. Even in terms of Townsend DMS spectra are distinguished for different bulk temperatures (see Fig. 1b).

The present study focuses on the temperature effect in differential mobility spectrometry. The general aim is to improve DMS spectral stability and repeatability under varying ambient conditions. We present experimental investigations of the temperature dependence of the DMS peak positions and an empirical physical model to represent the obtained experimental data. Our model can be used for temperature correction of DMS spectra.

* Corresponding author. Tel.: +1 781 457 5373; fax: +1 781 457 5399.
E-mail addresses: ekrylov@sionex.com (E.V. Krylov), scoy@sionex.com (S.L. Coy), egnazarov@sionex.com (E.G. Nazarov).

1387-3806/$ – see front matter © 2008 Elsevier B.V. All rights reserved.
doi:10.1016/j.ijms.2008.10.025

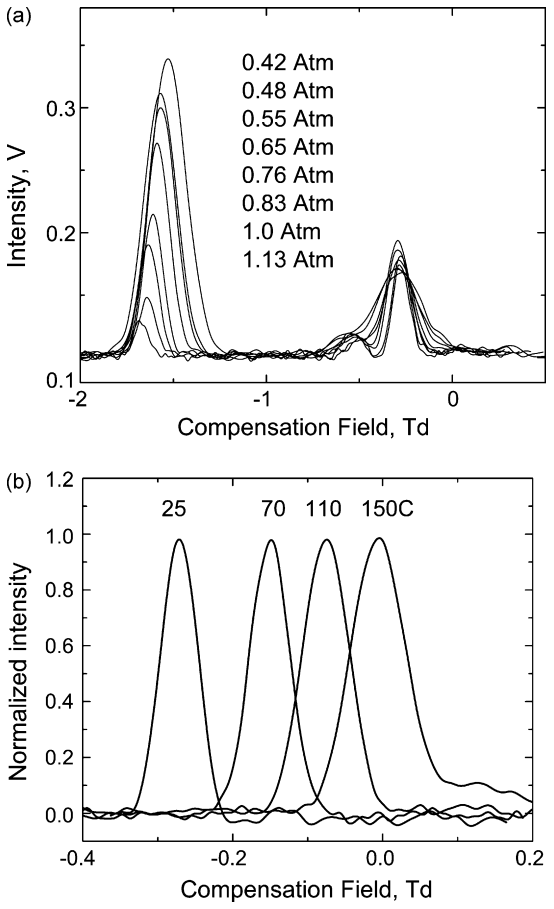

Fig. 1. Positive DMS spectra of methyl salicylate ions at the same 100 Td separation field, but with different drift gas pressures (a) and temperatures (b). Pressure does not affect the DMS spectrum scaled in Td units. Variation of peak position with temperature remains even after Townsend scaling.

We begin with a general review of ion mobility and differential mobility spectrometry. Section 3 describes the experimental setup, data collection and analysis. Then, an empirical model and generalized effective temperature capable of simplifying our observations is presented.

1. Ion mobility

The current understanding of ion mobility has been described in detail in [18,19] but we provide here a brief overview of the basic phenomena involved in our studies.

An electric field of strength E causes ions to move through a gas media of density N. Simple physical considerations, confirmed by calculations and experiments, show that the ion drift velocity is proportional to the parameter E/N through the coefficient of mobility, K. This result is exact as long as only binary ion–molecule collisions are important and many-body collisions are negligible. It was experimentally verified in our previous work [17]. If the electric field strength, E, changes proportional to density (or, equivalently, pressure for ideal gases), E/N remains unchanged and the coefficient of ion mobility processes is unchanged. This scaling rule had been proven to work well in DMS at fixed gas temperature.

To account for the gas temperature effect in DMS let us consider high field ion mobility in detail. Approximately constant ion mobility, defined as the ratio of velocity to field strength, is determined by the ion-neutral interaction at higher pressures. The high frequency of ion-neutral collisions (~30 GHz) causes ion velocity in a field to reach a limiting value rapidly. When the collision duration is much shorter than the time between collisions, the binary ion-neutral scattering momentum transfer, scaled by the collision rate, determines the ion mobility. Thus, the ion mobility depends on the ion-neutral interaction potential as well as the distribution of collision energies. If the energy gained by the ion from the electric field is small in comparison with the thermal energy, the mobility coefficient K is independent of E/N. In that low field case, the mean interaction energy does not differ significantly from the mean energy of thermal collisions.

At higher electric fields, ions acquire substantial energy from the field and the frequency and strength of the ion-neutral interaction changes. As a result, the mobility coefficient K at fixed bulk gas temperature becomes dependent on the electric field as shown in Eq. (1):

$$K\left(\frac{E}{N}\right) = K(0)\left\{1 + \alpha\left(\frac{E}{N}\right)\right\}, \quad (1)$$

where $K(0)$ is the mobility coefficient under low field conditions; $\alpha(E/N) \ll 1$ is nondimensional function characterizing the field mobility dependence (called the alpha function below); E/N is the electric field in Townsend (Td) units ($1\,\text{Td} = 10^{-17}\,\text{V cm}^2$). Under standard conditions (1 atm, 0 °C), $N_0 = 2.687 \times 10^{19}\,\text{cm}^{-3}$, so 1 Td corresponds to 268.7 V/cm.

Temperature affects the ion mobility in two distinct ways. Temperature changes gas density, N, and hence the value of E/N and the field contribution to ion kinetic energy. In addition, gas temperature changes the ion and neutral kinetic energy distributions and hence changes the distribution of ion-neutral collision energies and the ion mobility.

A fundamental analysis of the temperature dependence of ion mobility would require knowledge of the ion-neutral interaction potential. But an empirical generalization is still possible if we make use of the fact that temperature and field affect ion transport in the same way, by increasing ion-neutral interaction energy. The most important result of the two-temperature theory is a scaling rule which condenses the two variables T and E/N into the single variable, effective temperature, T_{eff} [20]

$$\tfrac{3}{2}kT_{\text{eff}} = \tfrac{3}{2}kT + \tfrac{1}{2}MV_{\text{d}}^2, \quad (2)$$

where T is the drift gas temperature in K, M is the drift gas molecular weight, V_{d} is the ion drift velocity, and k is Boltzmann's gas constant. For nitrogen drift gas, this becomes

$$T_{\text{eff}} \approx T + 8.09 \times 10^{-3} K_0^2 \left(\frac{E}{N}\right)^2, \quad (3)$$

where K_0 is the reduced coefficient of ion mobility in $\text{cm}^2/\text{V s}$, and E/N is electric field in Td. The reduced mobility is $K_0 = KN/N_0$, where K and N are observed values of the ion mobility and drift gas density; N_0 is the standard gas density. Reduced mobility has a reduced variation with pressure and temperature and is utilized for species identification in conventional ion mobility spectrometry [21].

When ions and neutrals are both atomic, so that only elastic collisions take place, the scaling rule works well. Temperature and field mobility dependences of the atomic ion in noble gases coincide in the effective temperature scale. The situation is more complicated for polyatomic ions and/or neutrals. In molecular systems we must account for inelastic collisions involving rotational and vibrational degrees of freedom. In high field conditions, inelastic collisions transfer energy between the different degrees of freedom and so influence the effective temperature. Lacking information on inelastic cross-sections, we can still combine T and E/N into a generalized $T_{\text{eff}}(T,E/N)$, with the expectation that a smooth inelasticity correction will allow the field and temperature dependences of the

mobility to coincide. Redistribution of energy between the different degrees of freedom is expected to reduce the energy in translational degrees of freedom because some of the field energy will go into the rotational and vibrational degrees of freedom, thereby reducing the effective temperature parameter, T_{eff}. This analysis serves to provide an interpretation of the experimental data and suggests some ideas for the data processing.

2. Differential mobility spectrometer

This section provides a short description of the differential mobility spectrometer and a mathematical representation of the phenomena involved.

In contrast with conventional ion mobility spectrometry based on the measurements of the low field, DMS ion separation is based on the ion mobility field dependence. The mobility field dependence ($\alpha(E/N)$ in Eq. (1)) is a characteristic feature of the ion-drift gas system and is employed for ion separation in DMS. In general, DMS exploits the effect of the elevated energy which ions obtain from the electric field. In particular, the DMS measures the difference in the mobility coefficient at high and low electric field strengths.

In DMS, ions in drift gas flow through a gap between two electrodes (called the "filter gap"). A high amplitude, high frequency, asymmetric waveform (separation voltage, SV) is applied to the electrodes to create an electric field (separation field, S). The ions undergo fast oscillation in response to the separation field. The ion displacements during the positive and negative portions of the zero-mean separation field differ slightly because of unequal mobilities at the high and low fields. As a result of this displacement, ions drift perpendicular to the gas flow, toward one of the electrodes. Ions pass through the gap between the electrodes only if the drift velocity is small enough to avoid reaching the electrodes and being neutralized. The ion drift velocity and direction depend on $\alpha(E/N)$, the separation field amplitude and separation field waveform.

Ions may be retained within the gap (i.e. compensated, with no net drift) by applying a quasi-static compensation voltage (CV) to the electrodes. The constant electric field (called compensation field, C) is superimposed on the separation field, and produces an offsetting drift, allowing ions to remain inside the gap. Ions with differing alpha functions pass through the gap at different compensation voltages. Scanning the CV produces a DMS spectrum of the ionic mixture (see Fig. 2a).

Compensation field, C, is related [12] to the alpha function, $\alpha(E/N)$, the amplitude of the separation field, S, and field waveform, f, by

$$C = \frac{S\langle \alpha f\rangle}{1 + \langle \alpha\rangle + S\langle \alpha' f\rangle}, \tag{4}$$

where α' is the derivative with respect to E/N, and triangular brackets denote the average over a period of the separation field.

For practical purposes Eq. (4) may be expanded in a series [9]. A power series expansion allows calculation of the DMS peak position from the alpha function of the ion. The inverse problem also can be solved: one can calculate the alpha function for the ion from experimental data.

The alpha function may be approximated as an even power series of the electric field strength. That polynomial form is consistent with symmetry considerations (i.e., an ion velocity value does not depend on the electric field direction) [3]:

$$\alpha\left(\frac{E}{N}\right) = \alpha_2\left(\frac{E}{N}\right)^2 + \alpha_4\left(\frac{E}{N}\right)^4 + \alpha_6\left(\frac{E}{N}\right)^6 + \ldots, \tag{5}$$

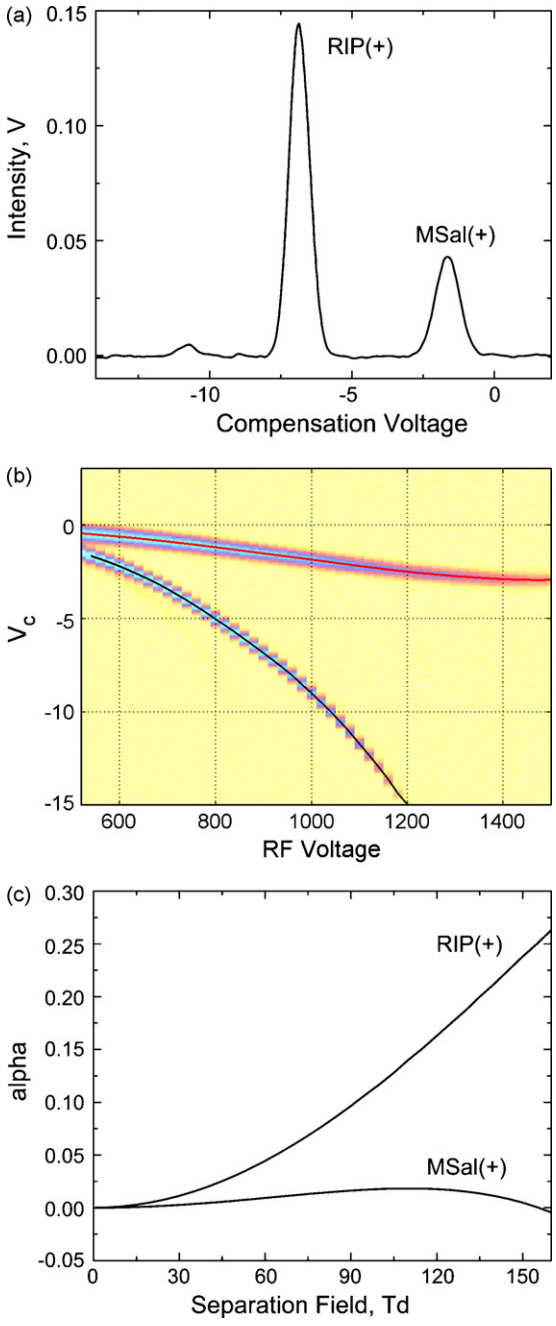

Fig. 2. Methyl salicylate positive ions. (a) DMS spectrum at 40 °C for SV = 900 V; (b) dispersion plot at 40 °C with derived peak positions; (c) alpha function of methyl salicylate cations and reactant ions derived from the dispersion plot.

where α_2, α_4,..., α_{2n} are series coefficients of the alpha function expansion. Series coefficients are definitively related to the corresponding alpha function.

DMS peak position dependence on the separation field, $C(S)$, is expanded in odd powers of the separation field, S:

$$C(S) = c_3S^3 + c_5S^5 + c_7S^7 + \ldots \tag{6}$$

Substituting the expansions for the alpha function and $C(S)$ into Eq. (3) yields a set of equations for the expansion coefficients [22]

$$\begin{aligned} c_3 &= \alpha_2\langle f^3\rangle \\ c_5 &= \alpha_4\langle f^5\rangle - 3c_3\alpha_2\langle f^2\rangle \\ c_7 &= \alpha_6\langle f^7\rangle - 5c_3\alpha_4\langle f^4\rangle - 3c_5\alpha_2\langle f^2\rangle \end{aligned} \tag{7}$$

where the separation waveform moments are defined by

$$\langle f^n \rangle = \frac{1}{T}\int_0^T f^n(t)dt \quad (8)$$

Eq. (7) may be used in both directions. Compensation field dependence and alpha function are unambiguously related to each other and may be computed, one from the other.

3. Experimental

3.1. Instrumentation

Peak positions for a few ions were observed in the Sionex microDMx planar DMS as a function of temperature and separation voltage. Experimental conditions covered the range from 25 °C to 150 °C at 1 atm. Temperature stability provided by the built-in controller was better than 1 °C. Pressure readings are also provided by the instrument and were used in computing the field expressed in Townsend units. Peak amplitude of the separation voltage was varied from 500 V to 1500 V in a planar DMS channel with height 0.5 mm, width 2 mm and length 10 mm. Thus, peak electric field in the analytical gap was 10,000 V/cm to 30,000 V/cm. Sionex uses a separation field calibration technique based on SF_6^- peak positions, with those positions determined as a function of field by direct high voltage waveform measurement. Purified nitrogen was used as a drift gas at typical flows of 5 cm^3/s resulting in ion residence time in the DMS sensor of 2.0 ms. Drift gas was dry nitrogen obtained from liquid nitrogen boiloff. Moisture was at sub-ppm levels as measured by Panametric Moisture Image and Michell Instruments moisture meters at the sensor outlet.

3.2. Ion species

We have analyzed DMS spectra for five molecular ions in nitrogen drift gas. The samples were ionized by a ^{63}Ni ionization source. Produced ions were identified by mass spectrometer. A DMS analyzer was joined to a mass spectrometer in a way based on the interface previously described in Refs. [16,17]. DMS sensor without detecting electrodes was connected to the API-MS inlet orifice. So ions from the DMS were directly introduced into the mass spectrometer (AccuTOF JMS-T100LC time-of-flight mass-spectrometer, JEOL, Peabody, MA). In the DMS–MS and DMS experiments we used the same gas and sample delivery systems. The ions that we have analyzed were

(1) Cations
- Toluene MH^+ and M^+ (m/z 93, 92).
- Dimethylmethylphosphonate protonated ions MH^+ (m/z 125).
- Dimethymethylphosphonate proton bounded dimer ions M_2H^+ (m/z 249).
- Methyl salicylate protonated ions MH^+ (m/z 153).
- Reactant ions $(H_2O)_nH^+$ (m/z 19, 37).

(2) Anions
- Methyl salicylate deprotonated ions $(M-H)^-$ (m/z 151).
- Reactant ions O_2^-, $(H_2O)O_2^-$ (m/z 32, 50).

A stable flow of vapor samples (DMMP or methyl salicylate) was provided either by diffusion sources or from Model 190 Dynacalibrator® calibration gas generators (VICI Metronics Inc., Poulsbo, WA) using permeation tubes were provided by Kin-Tek Laboratories, Inc. (LaMarque, TX). Supply lines after the vapor generator were kept at 80 °C to minimize sample adsorption. Peak positions were verified to have no dependence on concentration for the 1–10 ppb levels used in these measurements.

Toluene was supplied from gas cylinder with gas mixture of 10 ppm toluene and 1 ppm SF_6 in nitrogen (Scott Gases), and diluted at 1:200–1:300 ratios by the nitrogen drift gas. There is no dependence of peak position on mixing ratio, and the presence of SF_6 anion does not affect the toluene peak position at this concentration.

3.3. Data acquisition and processing

Software provided with the Sionex microDMx permits DMS spectra to be recorded, stored, and displayed for positive and negative ions simultaneously. Separation voltage can be stepped as compensation voltage scanned. The software allows the display of spectra as line plots of ion current vs. compensation voltage for a fixed separation voltage (see Fig. 2a), or as topographic plots scanned in both compensation and separation voltages [23]. This later option permits the creation of the topographic view of the CV(SV) dependence called the dispersion plot. The dispersion plot (see Fig. 2b) is generated by stepping the SV as CV is scanned. The range of SV was nominally 500–1500 V typically stepped in 10 V intervals. CV was scanned over an appropriate range to capture ion current for the target ion at all SV values.

Analysis software written in MATLAB (Mathworks, Natick, MA) was used to obtain least-squares-optimized values of peak positions (see Fig. 2b), peak widths and peak intensities at all separation voltages. The lineshape used in fitting DMS spectra was a modified triangular shape that more accurately represents the expected DMS lineshape including diffusion effects than a gaussian.

Origin 7.5 (OriginLab Corporation, Northampton, MA) was used for smoothing spectra, expanding the $C(S)$ dependences into the power series and drawing final plots. Excel (Microsoft Corp.) was used for calculation of the alpha functions (see Fig. 2c) and the effective temperature dependences (discussed below).

4. Results and discussion

The procedure applied to positive methyl salicylate ions is presented below as an example of our studies. Other molecular ions were analyzed in the same way.

Dispersion plot data were recorded at 13 temperatures (25 °C, 40 °C, 50 °C, 60 °C, 70 °C, 80 °C, 90 °C, 100 °C, 110 °C, 120 °C, 130 °C, 140 °C and 150 °C). CV(SV) dependences were extracted from the experimental data (Fig. 3a). Alpha functions were calculated from the CV(SV) dependences (Fig. 3b) as described above.

This data analysis provides normalized field mobility dependences for each temperature. We postulated the existence of a certain effective temperature variable condensing both field and temperature dependences. Using this effective temperature as abscissa, field ion mobility dependences should lay on a single smooth curve regardless of the bulk drift gas temperature.

Beginning from the lowest temperature, we reconstructed temperature mobility dependence as follows. Ion mobility, K, at the lowest temperature is assigned an arbitrary value. Mobility at the next temperature point will be

$$K(T_{i+1}) = K(T_i)\left(1 + \alpha_i\left(\frac{E_{i+1}}{N}\right)\right), \quad (9)$$

where $K(T_i)$ is ion mobility and $\alpha_i(E/N)$ is alpha dependence at temperature T_i; E_{i+1}/N corresponds to the temperature step $T_{i+1}-T_i$ according to our postulated equation for the effective temperature. This procedure computes the temperature mobility dependence within a constant factor. All temperature mobilities dependences calculated from experimental field mobility dependences in terms of effective temperature are expected to lay on the same curve.

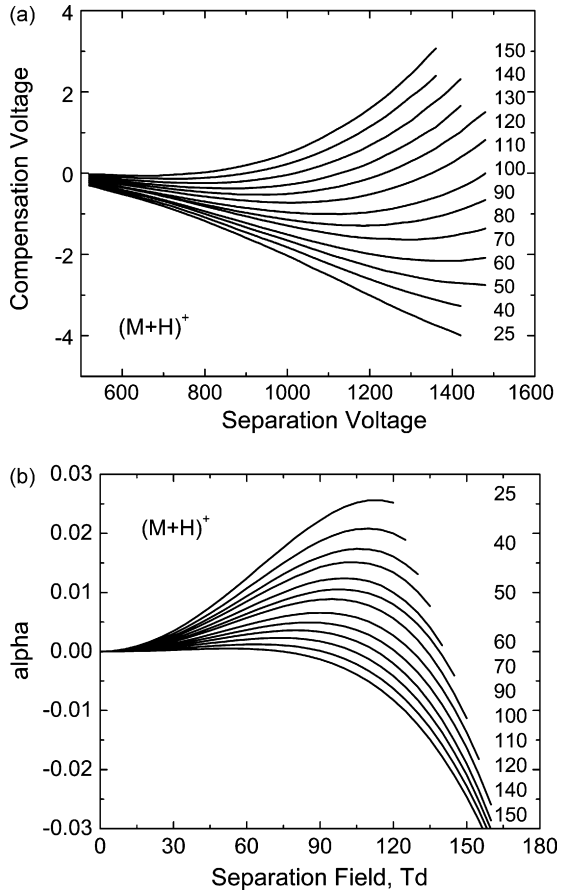

Fig. 3. (a) Compensation voltage vs. separation voltage for methyl salicylate cations for temperatures from 25 °C to 150 °C and (b) corresponding alpha function.

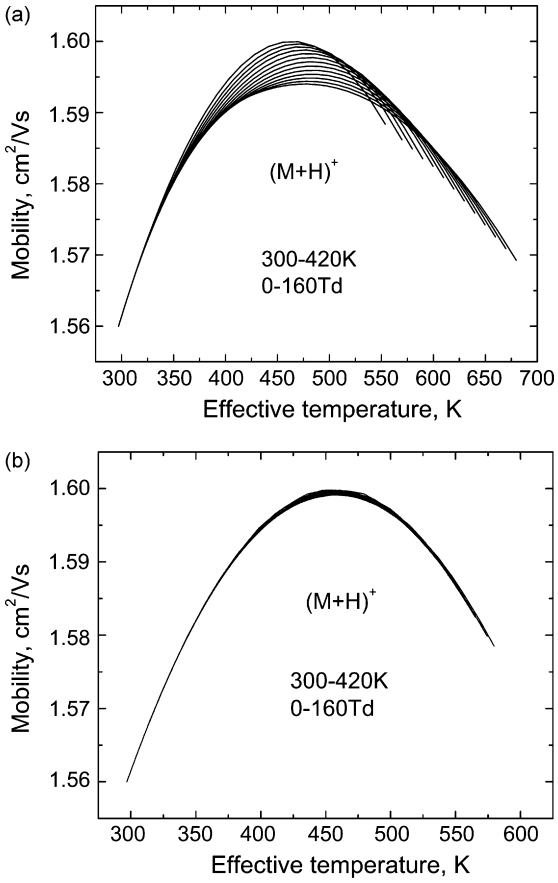

Fig. 4. Reduced mobility of methyl salicylate cation as a function of the drift gas temperatures using (a) classic effective temperature (Eq. (2)) and (b) effective temperature modified for inelastic collisions (Eq. (10)). Classic effective temperature does not allow experimental curves to fit each other.

Classic effective temperature equation (see Eq. (2)) results in the discrepancy between the experimental mobility curves (Fig. 4a). That is expected because the effective temperature was derived assuming conservation of momentum and kinetic energy at each collision. This assumption is not valid if the internal molecular degrees of freedom are involved in the ion-neutral interaction. In that case, electric field energy is redistributed between internal and external degrees of freedom and the effective temperature relation is disturbed.

To account for the influence of inelastic collisions, we modify the field part of the equation for classic effective temperature, T_{eff}, to include a coefficient $\zeta < 1$, a dimensionless factor which reduces the contribution of electric field to the effective temperature.

$$T_{\text{eff}} \approx T + 8.09 \times 10^{-3} \zeta K_0^2 \left(\frac{E}{N}\right)^2 \quad (10)$$

Using this equation, it is possible to condense the field and temperature dependences of the mobility into a single variable. The field and temperature dependences of the mobility coincide in a scale of the modified effective temperature if the energy loss ratio, ζ, is allowed to depend on the drift gas temperature (see Fig. 4b).

A fitting procedure is able to determine $h(T)$, the field-dependent part of the effective temperature including the coefficient ζ given by

$$\mathrm{h}(T) = 8.09 \times 10^{-3} \zeta(T) K_0^2 \quad (11)$$

Using $K_0 = 1.56\,\text{cm}^2/\text{V s}$ at 450 K for positive methyl salicylate ion (our own data obtained with DMS–IMS tandem instrument), and the obtained by fitting procedure $h(T)$ values, the ion mobility dependence on modified effective temperature can be restored as shown in Fig. 4b.

Thus the effects of field and temperature on ion mobility can be condensed into the modified effective temperature if the energy loss ratio is allowed to depend on the drift gas temperature. That may be interpreted as follows. As the collision energy increases with the gas temperature, internal degrees of freedom (rotational and vibrational) exchange energy with translational degrees of freedom. The field energy redistributes differently after a collision at higher temperature than at lower temperature because more energy is lost to excite the internal degrees of freedom. We have found that a single parameter, ζ, with smooth temperature dependence, is able to account for these effects empirically.

As noted in Eq. (11), reduced mobility appears only in combination with $\zeta(T)$, When reduced mobility is known from IMS measurements, the energy loss ratio can be computed from the fitting factor, $h(T)$. Fitting factors for all investigated ions are shown in Fig. 5a. If reduced mobility K_0 for the ion is known with sufficient accuracy, the energy loss ratio, $\zeta(T)$, can be estimated. Energy loss ratios as a function of the gas temperature are smaller than 1 and monotonically decreasing for all the ions that we have examined (see Fig. 5b). Reduced mobilities used for the calculations are presented in Table 1.

To verify our findings we compare our DMS experimental data with IMS experimental data on the temperature dependence of ion mobility. We plotted reduced ion mobility against modified effective temperature for all investigated ions in Fig. 6. Experimental data for the DMMP ions obtained with conventional IMS

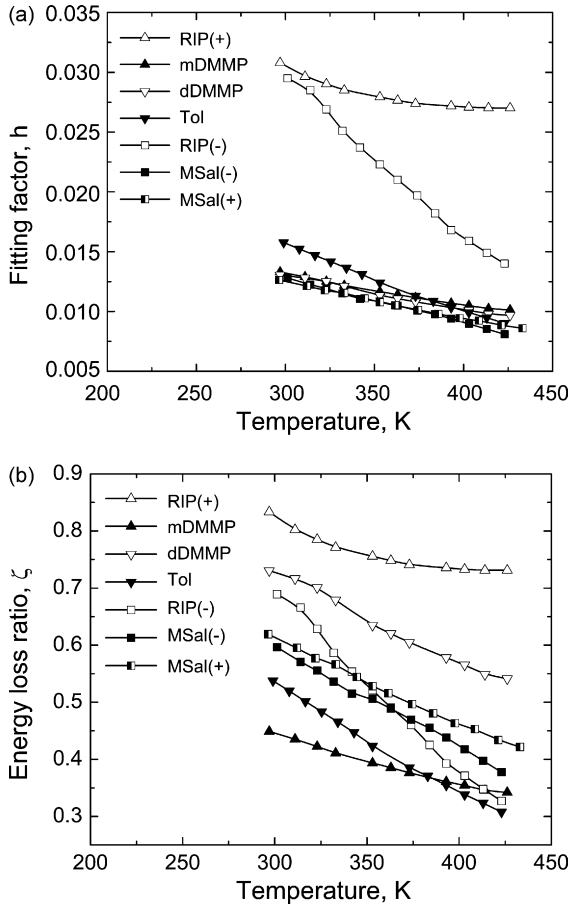

Fig. 5. (a) Fitting factor $h(T)$ as a function of gas temperature for various ions and (b) corresponding dependence of the energy loss ratio for molecular ions with known reduced mobility values.

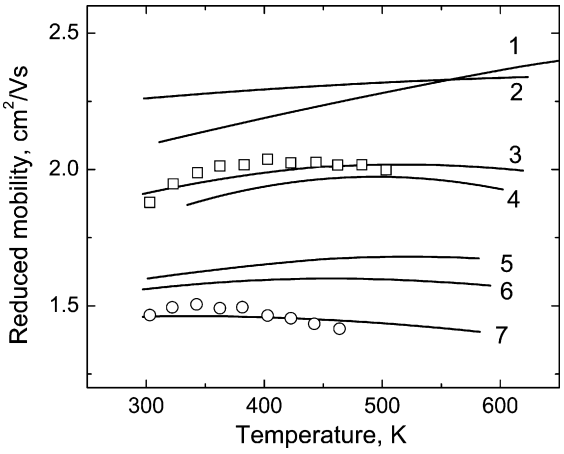

Fig. 6. Temperature dependences of reduced ion mobilities. Curves for DMS data (1—RIP(+); 2—RIP(−); 3—DMMP monomer; 4—toluene; 5—methyl salicylate (−); 6—methyl salicylate (+); 7—DMMP dimer). Points for IMS data are IMS mobility values recalculated from Fig. 2 of Ref. [25] (squares—DMMP monomer; circles—DMMP dimer).

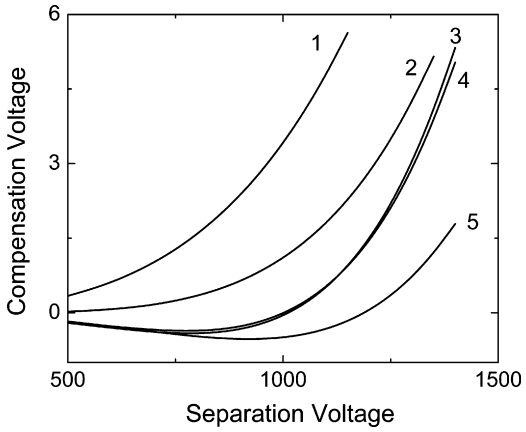

Fig. 7. Expected dispersion plots for investigated ions at 180 °C (1—DMMP dimer; 2—methyl salicylate (+); 3—toluene; 4—DMMP monomer; 5—methyl salicylate (−)).

(Fig. 2 in Ref. [25], drift time vs. gas temperature) allow computing of the reduced mobilities in dependence of the gas temperature. Our DMS data (curves 3 and 7 in Fig. 6) appear to be in a good agreement with published IMS data (squares and circles in Fig. 6). This result demonstrates the fundamental connection between the temperature dependence of reduced mobility from IMS and the field dependence of differential ion mobility from DMS. Fig. 6 also shows that the use of high fields in DMS is able to extend knowledge of reduced mobility values to higher temperatures than can be conveniently reached in IMS.

The fitting factor $h(T)$ for the observed molecular ions vary in similar ways: decreasing quasi-linearly from 0.015 to 0.01 as the gas temperature increases from 300 K to 450 K. That similarity allows development of an algorithm to correct DMS peak positions for variation of the carrier gas temperature. A general outline of the algorithm is as follows. Dispersion plot (compensation voltage against separation voltage) at lower temperature for target ions provides the mobility field dependence (alpha function). Under the proposed T_{eff} correction, one can restore the mobility temperature dependence and can recalculate alpha functions at elevated temperature. This alpha function may be utilized for computation of CV(SV) at elevated temperature for these ions. For example in Fig. 7 is shown the expected dispersion plots for investigated molecular ions at 180 °C. This algorithm may significantly improve the accuracy of the DMS instrument.

From a practical point of view, drift gas temperature may be stabilized by the DMS instrument sensor temperature control [23].

Table 1
Ion composition and reduced mobility values for ions studied in this work. Underlined values were used to determine $\zeta(T)$ factors.

Ion	Mass	Structure	Reduced mobility ($cm^2/V\,s$)			
			Exp [24]	Exp [25]	Our data	Appr [26]
DMMP monomer	125	$(M+H)^+$	1.91	1.88	1.66	1.66
DMMP dimer	249	$(M_2H)^+$		1.46	1.28	1.21
Methyl salicylate	153	$(M+H)^+$			1.59	1.53
Methyl salicylate	151	$(M-H)^-$			1.56	1.54
Toluene	93, 92	$(M+H)^+$, M^+	1.87		1.87	1.86
RIP (−)	32, 50	O_2^-, $H_2O{\cdot}O_2^-$			2.26	2.55, 2.26
RIP (+)	19, 37	$(H_2O)_nH^+$		2.1	1.88	2.89, 2.45

But for portable field applications or DMS instruments working in harsh ambient conditions temperature compensation may be very useful. Temperature correction will allow DMS operation at lower temperatures, decreasing DMS power consumption and increasing DMS resolving power without sacrificing stability.

5. Conclusion

Based on the systematic experimental data we have developed a model for the effect of temperature on DMS performance by the use of a simple modification to the classic effective ion temperature to account for inelastic collisions. For molecular ions moving in the molecular gases, we have modified the equation of the effective temperature by the addition of an empirical coefficient characterizing fractional energy loss due to inelastic collisions. This coefficient is able to condense ion mobility dependences on field and temperature into one dependence on effective temperature. In the context of differential mobility spectrometry, our findings allow prediction of the gas temperature effect on DMS peak positions. Applying correction for gas temperature and pressure variation to DMS spectra improves instrument performance by guaranteeing instrumental stability and repeatability.

Acknowledgements

The authors are very grateful for the assistance of the Sionex engineering team, especially Charles Martin who assisted in improving sensor designs.

References

[1] M.P. Gorshkov, Inventor's Certificate of USSR 966583 (1982) G01N27/62.
[2] I.A. Buryakov, E.V. Krylov, V.P. Soldatov, Inventor's Certificate of USSR 1485808 (1989) G01N27/62.
[3] I.A. Buryakov, E.V. Krylov, A.L. Makas', E.G. Nazarov, V.V. Pervukhin, U.Kh. Rasulev, Tech. Phys. Lett. 17 (1991) 60.
[4] R.W. Purves, R. Guevremont, S. Day, C.W. Pipich, M.S. Matyjaszczyk, Rev. Sci. Instrum. 69 (1998) 4094.
[5] G.A. Eiceman, E.V. Krylov, N.S. Krylova, E.G. Nazarov, R.A. Miller, Anal. Chem. 76 (2004) 4937.
[6] I.A. Buryakov, Talanta 61 (2003) 369.
[7] N. Krylova, E. Krylov, J.A. Stone, G.A. Eiceman, J. Phys. Chem. 107 (2003) 3648.
[8] G.A. Eiceman, E.V. Krylov, B. Tadjikov, R.G. Ewing, E.G. Nazarov, R. Miller, The Analyst 129 (2004) 297.
[9] E. Krylov, E.G. Nazarov, R.A. Miller, B. Tadjikov, G.A. Eiceman, J. Phys. Chem. A 106 (2002) 5437.
[10] G.A. Eiceman, R.A. Miller, B. Tadjikov, E. Krylov, E.G. Nazarov, J. Westbrook, P. Funk, J. Chromatogr. A 917 (2001) 205.
[11] A.G. Anderson, E.G. Nazarov, E.V. Krylov, R.A. Miller, S.L. Coy, PITTCON, Chicago, IL, 2007.
[12] I.A. Buryakov, E.V. Krylov, E.G. Nazarov, U.Kh. Rasulev, Int. J. Mass Spectrom. Ion Proc. 128 (1993) 143.
[13] A.N. Verenchikov, E.V. Krylov, V.B. Louppou, A.L. Makas', V.V. Pervukhin, V.A. Shkurov, in: V.V. Malakhov (Ed.), Chemical Analysis of Environment, Nauka, Novosibirsk, 1991, p. 127.
[14] D.S. Levin, J. Am. Soc. Mass Spectrom. 18 (2007) 502.
[15] A.A. Shvartsburg, F. Li, K. Tang, R.D. Smith, Anal. Chem. 78 (2006) 3706.
[16] S.L. Coy, E.V. Krylov, R.A. Miller, E.G. Nazarov, 55th ASMS Conference, Indianapolis, IN, 2007.
[17] E.G. Nazarov, S.L. Coy, E.V. Krylov, R.A. Miller, G.A. Eiceman, Anal. Chem. 78 (2006) 7697.
[18] E.A. Mason, E.W. McDaniel, Transport Properties of Ions in Gases, Wiley, New York, 1988.
[19] E.A. Mason, in: T.W. Carr (Ed.), Plasma Chromatography, Plenum Press, New York, 1984, p. 49.
[20] E.A. Mason, E.W. McDaniel, Transport Properties of Ions in Gases, Wiley, New York, 1988, p. 149.
[21] G.A. Eiceman, Z. Karpas, Ion Mobility Spectrometry, CRC Press, Boca Raton, 1994, p. 191.
[22] E.V. Krylov, E.G. Nazarov, R.A. Miller, Int. J. Mass Spectrom. 226 (2007) 76.
[23] SVAC Series Product Manual, S-400003-00, Revision H, 2005, Sionex Corporation Inc.
[24] N. Agbonkonkon, H.D. Tolley, M.C. Asplund, E.D. Lee, M.L. Lee, Anal. Chem. 76 (2004) 5223.
[25] M. Tabrizchi, F.J. Rouholahnejad, Phys. D: Appl. Phys. 38 (2005) 857.
[26] H.E. Revercomb, E.A. Mason, Anal. Chem. 47 (1975) 970.